UNCLASSIFIED

AD NUMBER
AD215773

CLASSIFICATION CHANGES	
TO:	UNCLASSIFIED
FROM:	CONFIDENTIAL

LIMITATION CHANGES
TO: Approved for public release; distribution is unlimited.
FROM: Distribution authorized to U.S. Gov't. agencies and their contractors; Administrative/Operational Use; 25 NOV 1958. Other requests shall be referred to Department of the Army, Attn: Public Affairs Office, Washington, DC 20310.

AUTHORITY
ATRC ltr 24 Mar 1967 ; ATRC ltr 24 Mar 1967

THIS PAGE IS UNCLASSIFIED

Armed Services Technical Information Agency

ARLINGTON HALL STATION
ARLINGTON 12 VIRGINIA

| FOR
MICRO-CARD
CONTROL ONLY | 1 | OF | 2 |

CONVOPLANE PRELIMINARY DESIGN STUDY,

MODEL CONSTRUCTION,

AND WIND TUNNEL TEST

GER-8763, Rev B

25 November 1958

Contract DA44-177-TC-437

Goodyear Aircraft Corporation

Akron 15, Ohio

DISCLAIMER NOTICE

UNCLASSIFIED
Technical
Report

Defense
Technical
Information
Center

DTIC

UNCLASSIFIED

THIS DOCUMENT IS BEST
QUALITY AVAILABLE. THE COPY
FURNISHED TO DTIC CONTAINED
A SIGNIFICANT NUMBER OF
PAGES WHICH DO NOT
REPRODUCE LEGIBLY.

GER- 8763 REV. B.

DATE November 25, 1958

REF NO. _____

GOOD/YEAR

GOODYEAR AIRCRAFT CORPORATION

AKRON, OHIO

CONVOPLANE PRELIMINARY DESIGN STUDY, MODEL
CONSTRUCTION, AND WIND TUNNEL TEST
Contract No. DA 44-177-TC437

The Findings and Recommendations Contained in
this Report are those of The Contractor, and
do not necessarily reflect the views of The
Chief of Transportation.

This Report shall not be reproduced in whole
or in part without the written consent of The
Chief of Transportation

24 Ind. 5 June 59
TCPEC-TS-I
(6 Apr 5?)

REVISIONS

REMARKS

REV	DATE	MADE BY	APPD BY	PAGES AFFECTED	REMARKS
A	4/30/58			Added: Frontispiece Rev: 111, 23, 25	
B	11/25/58			Completely Revised	

2119-51A (1-58)W

The Goodyear Aircraft Convoplane in Army Operations

TABLE OF CONTENTS

INDEX TO FIGURES

77-108 (1-53)M

TABLE OF CONTENTS (CONT'D)

TABLE OF CONTENTS (CONT'D)

SUMMARY

The purpose of this program was to determine the feasibility of the Convoplane concept and define its aerodynamic characteristics.

The Convoplane concept may be defined as an aircraft that combines the high speed forward flight of a conventional airplane with the hovering ability of a helicopter, without changing the attitude of the aircraft itself or any of its major components.

The concept takes its form in the shape of a buried rotor surrounded by ducting in such a manner that either hovering flight or forward flight conditions are permissible.

By entirely enclosing the rotor system within the wing. The Convoplane attempts to obtain hovering efficiencies which are considered good for helicopters and at the same time get forward flight speeds which are greater than those possible for the helicopter.

The results of the wind tunnel tests, conducted by the Goodyear Aircraft Corporation under the auspices of the U. S. Army Transportation Research and Engineering Command, presented herein indicate that this is possible. At the same time the test results demonstrate that these conditions are obtainable in a vehicle which utilizes one basic propulsion system to obtain hovering flight through transition to forward flight by means of ducted airflow rather than by turning either the propulsion system or the vehicle itself.

Although the main purpose of this program was to demonstrate feasibility by obtaining basic research data, it will also be shown that substantial improvement of the system is now possible with the information collected as a result of these tests.

LIST OF SYMBOLS

q = Dynamic Pressure at the Rotor Disk (Lbs/Ft^2)

q_t = Free Stream Dynamic Pressure (Lbs/Ft^2)

q_i = Inlet Dynamic Pressure (Lbs/Ft^2)

q_E = Dynamic Pressure at Exit Nozzle (Lbs/Ft^2)

Δq_H = $q_e - q_i$

A = Rotor Disk Area (Ft^2)

A_1 = Inlet Area (Ft^2)

A_e = Exit Nozzle Area (Ft^2)

D = Rotor Diameter (Ft)

D_M = External Drag (Lbs)

F_{100} = Thrust when doors are 100% open and the model is in the hovering condition.

F_n = Thrust vector obtained when doors are in any intermediate position, including fully closed

H = Total Pressure Head (Lbs/Ft^2)

$H.P.$ = Input Horsepower calculated from input torque

HP_R = Horsepower required

J = Rotor Advance Ratio

L = Lift (Forward Flight) (Lbs)

M = Rotor Figure of Merit

N = Rotor revolutions/Min.

P = Static Pressure Head (Lbs./Ft^2)

Q = Input Torque (Ft-Lbs) Measured at rotor hub

Q_F = Volume of Air Flowing/ Unit of Time

* Balance of Symbol's on Page 69 ,pull out when reading text.

SECTION I. INTRODUCTION

The helicopter has evolved as the first practical demonstration of
a vertical lift device, but whose forward speed capabilities are
limited mainly because of compressibility effects at the tips of the
advancing blades and stalling at the inboard part of the retreating
blades because of high angles of attack.

In order to extend the forward speed range of the helicopter, and
yet retain the vertical lift advantages, many ingenious ideas have
been advanced. Some of these ideas have been realized in the form
of actual full scale flight vehicles. At one end of the spectrum
are those devices which either utilize additional propulsion systems
or turn the propulsion system to obtain various modes of flight. On
the other end of the spectrum is the high speed jet type aircraft
with sufficient thrust to weight ratio which permits it to hover and
rise vertically. Transition to forward flight is usually accomplish-
ed either by rotating the fuselage or by rotating the propulsion
system and/or ducting the air through a 90° turn. Many other con-
figurations have been evolved between these two extremes.

Since it is difficult to improve on the helicopter as a vertical
lift device and, in the same sense, since a wing is a very efficient
lift device in forward flight, a system was devised utilizing both of
these approaches which it was felt would achieve transition from hover-
ing to relatively high speed forward flight with one power source and
no rotation of either the airplane or the rotor axis.

The system so devised was in general to bury the rotor within the
wing, with the rotor shrouded in such a fashion that the air passes
through it axially regardless of the flight regime of the aircraft.
In hovering flight, louvres in the top and bottom wing surfaces are
opened, allowing air to pass through the ship vertically. To
accomplish transition, the louvres are closed in a pre-determined
sequence and rotation of the thrust component is obtained by a
change in the direction of the airflow. In forward flight, the air
essentially, enters at the leading edge, passes through another
series of turning vanes into the rotor, then through another series
of turning vanes and exits at the trailing edge. Thus, the airflow
providing the thrust would be changed the necessary 90° to permit
transition from vertical flight to forward flight, and vice-versa.
Figures 1 and 2 depict the flow path during hovering and forward
flight conditions.

Since no experimental or theoretical data was available on which
to base engineering estimates, no specific performance for such a
vehicle could be entirely evaluated.

As a result, the program now concluded was sponsored by the U. S. Army Transporation Research and Engineering Command to obtain data which could be used for an evaluation of the performance of such a vehicle.

The program was planned to follow three basic steps. The first portion covered a preliminary configuration analysis of the flying test bed. Using the theoretical data obtained from this effort, the requirements for the wind tunnel test model were established. The second portion involved the design, fabrication, and testing of the model and analysis of the test results in terms of model data. Finally, the test data was interpreted in terms of test bed horse-power required and forward velocity attainable.

SECTION II. PRELIMINARY CONFIGURATION ANALYSIS

A. CONFIGURATION PLANFORM & AIRFOIL SELECTION

Preliminary effort was expended in determining a feasible planform
geometry for the overall configuration. Tailless and conventional
configurations were analyzed in conjunction with rectangular and
delta wing planforms to determine subsequent power requirements.

For the tailless configuration it was necessary that the rotor axis
be on or near the c.g. for hovering trim, and that the wing a.c. be
on or aft of the c.g. for forward flight. Incorporation of rectan-
gular planform would necessitate excessive wing areas to satisfy
the above two requirements. This results from the fact that the
centerline of the rotor is placed at approximately the 25% chord
which means that the rotor occupies 50% of the wing chord. The
remaining 50% of wing chord, and its correspondingly large area
are just to stabilize the configuration.

FORWARD   STABILIZING AREA   AFT

25% CHORD   50% CHORD
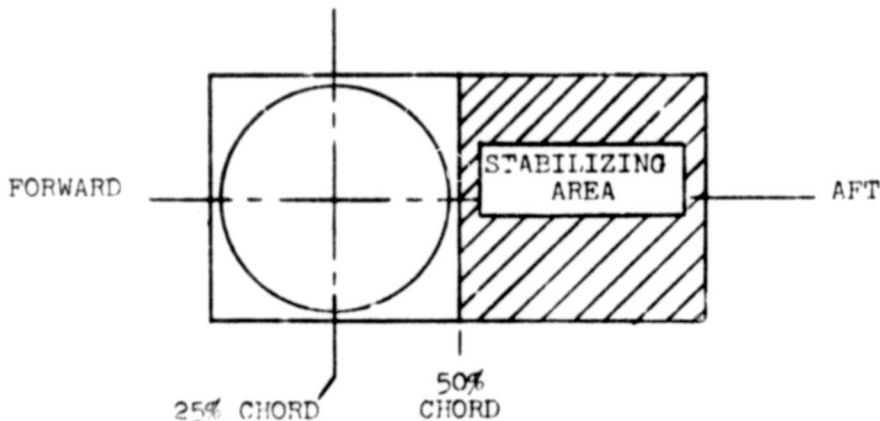
An increase in wing aspect ratio will be accompanied by a desir-
able rearward shift of the a.c., but would be offset by the in-
crease in wing area and a corresponding increase in power require-
ments.

A similar relationship can be shown to exist for the delta wing planform. An inherent advantage of this type of planform is the more aft location of the a.c., however, assuming the inlet geometry requires that the rotor circle be inscribed in a square whose front corners cannot protrude beyond the wing's leading edge, a further increase of the ratio of wing to disk area results.

The weight and power requirements necessary for this type of configuration suggested its abandonment in favor of a more conventional layout consisting of a wing and separate aft-mounted stabilizing surfaces. A few of the more notable advantages of the tailed configuration over the tailless design are:

1. The area required for stabilizing purposes need be only one-fourth the wing area.

2. The power requirements for hovering are considerably less.

3. A proportionate decrease in gross weight and drag;

4. A more convenient location of the c.g. and rotor center on the wing chord.

It is believed that the thick airfoil section necessary to house the rotors, ducting, and engines will not be appreciably detrimental in drag. Because of the flow through the airfoil it is felt that the drag wake will be appreciably changed to yield a total drag less than would be realized if there were no flow. It is further believed that a thinner airfoil section with flow would not yield a total drag much less than that of a much thicker section with flow.

B. ESTIMATED PERFORMANCE

The performance requirements for the flying test bed were determined based on obtaining a maximum speed of 200 MPH at an altitude of 6,000 feet. Dual-rotor configurations of aspect ratio 1.55 were considered throughout the study. Rotor diameters from 10 feet to 25 feet in diameter were investigated, but in each case the rotor housing was of minimum size to house that pair of rotors. A propulsive efficiency at 200 MPH of 0.65, as estimated by internal flow analysis for these conditions, permits presentation of power requirements in terms of gross or installed horsepower.

Figure 3 presents the curves of horsepower required to hover at varying gross weights for three rotor diameters. These curves are based on the assumptions that a nominal figure of merit of 0.65 can be attained. With proper blade design this efficiency will not reduce with increasing disk loading.

Figure 4 presents the gross horsepower required to meet the forward flight requirements for rotor diameters from 10 feet to 25 feet at three wing loadings. This curve is based on the assumption that all

4

the necessary aerodynamic lift is produced by the rotor housing at cruising speeds.

From these curves, a curve of allowable gross weight in hovering can be computed based on the power required for a forward flight speed of 200 MPH. Figure 5 presents this analysis in solid line curves. Superimposed upon the allowable lift curve is the estimated test bed weight curve. It is seen that a deficiency in hovering lift occurs at below a 14.5 ft. rotor diameter because the horsepower required to hover exceeds the forward flight horsepower while a surplus of lift occurs above this diameter.

The Convoplane concept is intended to present a shrouded rotor operating at or near normal helicopter disk loadings, but capable of higher maximum speed. Hovering load carrying capabilities at rotor diameters in excess of 14.5 ft. are higher than the nominal weight when power is limited by forward flight condition.

As determined from Figure 5 the load carrying capabilities at hover for a 18 ft. diameter rotor will exceed 30% of the nominal gross weight. This allows the versatility in operation considered desirable by the military.

C.   PROPOSED FLYING TEST BED

The wind tunnel model was based on the preceding configuration analysis. The results and conclusions of the wind tunnel tests are presented in Sections IV and V.

Essentially, the characteristics established in paragraphs A and B are still the primary goals for the test bed, but based on the propulsive efficiencies obtained from the current wind tunnel tests, a vehicle capable of 145 MPH is feasible instead of the 193 MPH predicted. This of course assumes no further internal flow improvement.

Figure 6 shows the predicted forward speed based on theoretical propulsive efficiencies, and the forward speed obtained on the basis of efficiencies derived from test results.

Table 1 gives an estimated weight breakdown for the test bed and Figure 7 is a three view drawing showing the general configuration of the test bed.

The general specifications recommended for the flying test bed are:

              Span   - 41 ft.
              Rotor Dia.   - 18 ft.
              No. of Passengers   - 2
              Estimated Weight   - 7598 lbs.
              No. of engines   - 2 - T58-GE-6 1050 S.H.P. ea.
              Forward speed   - 145 - 193 MPH

TABLE I

PROPOSED CONVOPLANE TEST BED WEIGHTS

ITEM	WEIGHT (Lbs.)
1. Engine Section (Engines, mounts, shafts, cooling ducts, lubricating system, fuel system, rotors)	1569
2. Fixed Equipment (Instruments, controls, communications, furnishings)	114
3. Structure	
a. Tail Group (Horizontal tail, rudders, booms)	487

b. Body Group
       (Ailerons, crew pod, rotor support
       booms, leading and trailing edge
       beams, center section, tip ribs.)
	1591

c. Body Group (Cont'd)
       (External skin and fairings, doors,
       door operating mechanism, turning
       vanes, rotor ducting)
	2577

d. Landing Gear	120

e. Pay Load
       (Crew, fuel, oil, cargo (test
       inst.)
	1140

TOTAL	7598 lbs.

SECTION III. DESCRIPTION OF WIND TUNNEL MODEL, TEST EQUIPMENT AND WIND TUNNEL TESTS

An attempt was made to design a model which would contain a large degree of flexibility in order to yield sufficient test data which would permit the necessary variables to be evaluated for the eventual design of a flying test bed.

A rotor system was incorporated that was capable of simulating the use of either single or multiple rotors. In each of the two rotors, either single rotation or counter-rotation could be used. The rotor hubs were so designed that a minimum of two blades or a maximum of six blades could be installed, thus permitting the evaluation of a large range of rotor solidities. Collective pitch change of the blades was provided for in the hub design in order that various blade angles could be investigated.

For simplicity of construction, the cross section of the blades was of a Clark Y shape with constant chord. A varying twist of 19° from root to tip was incorporated.

In order to assure axial flow through the rotors at all times, a set of turning vanes was installed both above and below the rotors.

A series of movable doors or louvres were placed in the upper and lower wing surfaces above and below the turning vanes. These doors were adjustable from full open to full closed. The power system consisted of a hydraulic motor driving through a gear box and timing belt arrangement to the rotors

The instrumentation for evaluating the internal flow characteristics consisted of total head and static head tubes placed throughout the model. They were installed in the inlet at the front of the model, above the rotors, below the rotors, at the exit in the rear of the model and on the upper and lower doors. The pressures were either picked up on manometer banks or through a scara-valve into an oscillograph.

Torque measurements were taken from strain gauges mounted in the hub of each rotor and recorded on an oscillograph. The strain gauges were mounted so that the torque imparted to each rotor did not involve the hydraulic motor or gear box. Much of the data was then taken from the oscillograph tape and processed through IBM machines.

Figures 8 through 17 show the model, its components and the instrumentation arrangement.

The wind tunnel program was divided into two parts. The internal flow evaluation was made at the Goodyear Aircraft 43" by 61" wind tunnel while the force measurements or external flow evaluation was made at the University of Detroit 10' by 7' wind tunnel. The reason for this was the desire to test the largest possible rotor size, which was too large for aerodynamic tests in the GAC tunnel. Since the configuration was not considered optimum, no attempt was made to evaluate it as such. The main effort was expended in trying to determine how the model reacted to different modes of flight.

Several arbitrary decisions were made in designing the model. When the doors or louvres were full open, it was assumed that the rotor acted in a manner similar to a helicopter in the hovering condition; drawing air from above through the rotor. When the louvres were full closed, then the air had to enter the rotor from an inlet in the leading edge of the wing and leave at an exit in the trailing edge. Arbitrarily, the inlet was made 25% of the rotor area and the exit was made 60% of the inlet area. By leaving the doors above and below the rotor open at partial settings, it was possible to obtain almost any ratio of inlet and exit area desired.

Some of the pertinent data for the model is as follows:

Span	41.00 inches
Chord	27.50 inches
Wing Area	1127.50 inches^2
Rotor Dia.	18.00 inches
Rotor Area/Rotor	1.765 Ft^2
Inlet Area	.476 Ft^2
Exit Area	.294 Ft^2

SECTION IV. DISCUSSION OF TEST RESULTS

A. INTERNAL AERODYNAMICS

In the GAC tunnel, the internal ducting was the only item under consideration and the tunnel acted only as a source for ram air. The tests were divided into two parts. Part one covered hovering flight conditions and part two covered forward flight conditions. The results of the hovering flight tests will be discussed first.

Since the air flow through the Convoplane in the hovering attitude encounters a set of doors and a set of turning vanes, both above and beneath the rotors, it was necessary to determine the penalty paid for this flow condition. At the same time it was desired to evaluate the effect of various rotor configurations. Therefore, rotor configurations consisting of (A) 2-blades-single rotation, (B) 4-blades-single rotation and (C) 2-blades-counter rotation were selected. Each of these configurations were tested in turn with turning vanes and doors in; turning vanes in, doors out; and turning vanes and doors out.

Actually, rotor configuration (A) was necessitated by the fact that the model tests conducted at the University of Detroit were done with 2-blades-single rotation. This was a result of blade damage suffered at the beginning of the test program and the fact that replacement blades were not available in time to install for further testing. In order to get correlation between the tests at the University of Detroit and GAC it was necessary to include this configuration on the GAC schedule.

Using the results of the tests conducted at the University of Detroit as a guide, it appeared that a blade angle setting of 10° produced the best results. A few preliminary runs at blade angle of 15° and 6.5° verified this. At 15° a reduction in effectiveness of the rotor was apparent and at 6.5° high enough disk loadings were not possible for the rotor speeds used. It should be pointed out, however, the blade angle of 10° may not be optimum, but did yield data representative of the rotor performance. When speaking of blade angle setting in this report, this will be the angle at the 75% radius of the blade.

Figure 18 shows power loading vs disk loading values obtained at a blade angle setting of 10° with doors and vanes in for the three

rotor configurations. Figure 19 is a similar curve with doors and vanes out. No curve appears for the doors out, vanes in condition because analysis of test results showed that less than 2% difference in disk loading and power loading was obtainable and it could be concluded that little penalty was suffered because of the presence of doors in the path of the air flow during hovering. Throughout the range of disk loadings tested less than one pound per horsepower had to be sacrificed for the presence of both the doors and turning vanes with the turning vanes making the principle contribution to this penalty.

It appears that for the range tested, increasing the number of rotor blades from two to four blades shows a slight improvement in the power loading vs disk loading curve with a more substantial improvement appearing when counter rotating rotors are used. It should be pointed out that when counter-rotation was used, both the upper and lower blades were set at the same blade angle. This resulted in the lower rotor absorbing approximately .9 the horsepower of the upper rotor. Improved performance could probably be obtained here if the upper and lower blade angles were chosen so that both rotors absorbed equal amounts of horsepower.

At this time a word should be said about torque readings. Throughout the test program, torque readings were taken at the rotor hubs. The readings appeared to be quite consistent for any particular blade angle setting and RPM combination regardless of whether the model was in hovering or forward flight with or without the tunnel operating. In other words, any particular combination of rotor blade angle and RPM gave, for all practical purposes, one reading for the range tested. Figure 20 is a plot of horsepower vs RPM for the three rotor configurations used and represent the horsepower values used in calculating power loadings and efficiencies in this report. This was permissible since it appeared that the rotors were oblivious to the flight attitude of the system, their power requirements being dictated by their particular setting.

The disk loadings and power loadings were obtained in the following manner.

1. q values measured beneath the rotor when averaged yielded the disk loading directly in $\#/ft^2$.

2. The hovering thrust was defined by $T = Aq$ where $A =$ rotor disk area; $q = \#/ft.^2$ of disk area.

3. Power loading was then obtained by dividing the thrust in pounds by the horsepower calculated from the torque for that particular setting.

4. Horsepower was calculated from the standard equation.

$$HP = \frac{Q \times RPM}{5252}$$ where Q = Torque in Ft. - lbs.

Forward flight conditions were investigated using a two-blade-single rotating rotor and a two-bladed-counter-rotating rotor configuration. Time did not permit any forward flight tests involving the four-bladed-single rotating arrangement. The purpose of the forward flight tests was to determine the overall propulsive efficiency of the propulsion system and to determine the internal flow efficiency, which accounts for the losses due to the presence of the turning vanes, rotor, inlet, exit, etc. The tests were run over a range of $\frac{V_0}{ND}$

values from .24 to 1.20. The tunnel speed Vo ranged from 30 MPH to 140 MPH, rotor speed was from 5000 to 10,200 RPM, depending on the configuration used.

Figure 21 shows a plot of efficiency (η) vs $\frac{V_0}{ND}$ for a 2-bladed

single rotating rotor. Maximum overall efficiency with this configuration is about 15.5%. The efficiency of the internal ducting system appears to about 18.5%. The low efficiencies for this particular rotor configuration was expected, since the entire propulsion system was designed on the basis of a 2-bladed counter-rotating configuration. As was mentioned earlier, it was necessary to test this configuration in order to obtain correlation with the University of Detroit tests.

Figure 22 shows a plot of efficiency vs $\frac{Vo}{ND}$ for a 2-bladed counter-

rotating rotor. It will be noted here that the overall propulsive efficiency shows a marked improvement, being about 30.5% while the internal flow efficiency is about 35%.

Since the configuration tested did not represent optimum, the efficiencies obtained demonstrate the feasibility of this propulsive concept. It can be implied from these two curves that when the optimum arrangement is obtained much better efficiencies will be available.

During transition from hovering to forward flight, intermediate door openings were arbitrarily chosen. These were in terms of % of disk area. The first condition was 75% of the disk area and the second 50% of the disk area. Figure 23 represents a relationship between the force vector obtained in hovering and the force vector obtained from any intermediate door opening to doors full closed. The solid line of Figure 23 represents the relationship when the doors were programmed as outlined above. A sharp drop off was observed down to the 75% setting, then a more gradual drop from this point to the doors full closed condition.

Earlier in this report it was mentioned that total and static head
tubes were located in the model at the inlet and exit, and before
and after the rotors. Figure 24 shows the location of these tubes
as they appeared in the model. Figures 25, 26, and 27 are examples
typifying the pressure distribution across the inlet, above the rotor,
below the rotor, and at the exit. Figure 28 is an example of the
type of pressure change that occurs through the ducting system as
blade angle of attack is changed. Figure 29 shows a variation of
pressure with power input. Examination of the curve shown in Fig-
ure 28 shows agreement within 5% of the volume of air flowing
through the inlet as compared with the volume of air flowing out of
the exit. The same is true of the flow through the upper rotor as
compared with the flow out the exit. It is when the flow below the
rotor is compared with the exit flow that a discrepancy appears.
Here the correlation is only within 30%. Based on these test results,
it appears that the lower rotor blades are not fully effective at
the tips. Assuming, for a moment this is the case. a calculation
was made in order to determine the effective area. It was found
that the blade radius of the lower rotor could be reduced by app-
roximately one (1) inch. This in turn would permit the ducting
shape to be modified. If further testing proves this condition to
actually exist, the proposed modification should also result in a
more efficient power input.

Figure 25 shows that the pressure distribution across the inlet and
exit is reasonably good. Examination of Figures 26 and 27, show
that the pressure point readings across the rotors, both above and
below is somewhat erratic. This was probably due in part to some
faulty pressure taps, but it is believed that most of the cause
could be attributed to the fact that the model was not operating
at the optimum blade setting and that the optimum arrangement for
the turning van , was not established as yet. Due to the fact
that a large portion of the pressure instrumentation was destroyed
by blade damage this area was not investigated further. Since de-
termination of feasibility was the main objective, temporary pres-
sure taps were later placed beneath the rotors in order to obtain
sufficient data for analyzing hovering flight.

As previously mentioned, Figure 24 is a diagram showing the location
of the pressure tubes in the model. Since the velocity in a duct
is seldom uniform across any section, and since a static and total
tube indicate velocity at only one location, a traverse is us-
ually made to determine the average velocity so that flow can be
computed. In general, the velocity is lowest near the edges or
corners, and greatest at or near the center. In the case of a
circular duct it was recommended that not less than twenty be used
along two diameters at centers of equal annular areas. Because of
the unusual amount of additional equipment in the ducting, it was
believed that additional traverses at 45° would be advantageous.
In determining the average velocity in the duct from the readings

12

given, the calculated individual velocities or the square roots of the velocity heads must be averaged. It is incorrect to use the average velocity head for this purpose since a square root relationship is involved in this calculation. Therefore, the dynamic pressure q was determined as follows:

$$q_{avg.} = \frac{\left[\sqrt{H_1 - P_1} + \sqrt{H_2 - P_2} + \ldots + \sqrt{H_n - P_n}\right]^2}{n}$$

where $H =$ Total pressure

            $P =$ Static pressure

In the brief time remaining in the test program, it was desired to run a few check points in order to demonstrate that improvements could be made in the forward thrust, when the doors were fully closed, and that a more advantageous door closing program could be obtained that would provide a larger available force vector during transition.

Since a large number of door settings relative to each other result in a given percentage of disk area, these settings may be quite arbitrary. So two intermediate points were once more picked. The doors were each set $20°$ and $40°$ from the full open position which gave 88% and 55% respectively for the door open area to disk area.

The dotted line in Figure 23 represents the change in $\frac{Fn}{F100}$ value. It will be noted that a more advantageous condition was created down to the 50% position. In order to improve that region between 50% and full closed, it was decided to attempt to show that the forward flight condition can be improved. Definite improvement was shown when the counter-rotating configuration was used. Further analysis of the flow conditions beneath the rotor showed that a starved condition appeared at the aft end of the rotor. Since it has been theorized that this condition might exist and that it might be necessary to operate at all times with some of the aft doors open, the last three doors were partially opened. An immediate increase in thrust was noted. The improvement by changing the rotor configuration and the last three door openings is shown by the dashed line in Figure 23.

As previously mentioned, rotor blade damage occurred during test operations at both the GAC tunnel and at the University of Detroit tunnel. Chronologically the failures occurred as follows:

1. At Goodyear Aircraft Corp. 1-9-58

2. At Goodyear Aircraft Corp. 1-14-58

3. At University of Detroit 2-6-58

4. At Goodyear Aircraft Corp. 3-12-58

The procedure followed up to the time of failure Number 1 was as follows:

(a) Tunnel was brought up to speed and permitted to stabilize.

(b) The model was then brought to power and the recording of test data started.

This procedure was decided upon prior to the beginning of test operations because it was observed that the transmission had a tendancy to heat up. It was on the seventh run with the tunnel operating at 150 m.p.h. and the model being brought to 7500 r.p.m., that a sudden clattering was heard such as when a rotating metallic object comes in contact with another object. Both the tunnel and model were immediately shut down. Upon examination of the model, it was discovered that the one blade in the upper rotor was bent and twisted and the other blade was damaged in a similar matter but to a much lesser degree. In addition, fifteen (15) of the thirty-two (32) static tubes were damaged beyond repair. After analyzing the situation it was decided that by using the method described for bringing the tunnel and model to speed that an unusual loading condition was placed on the blades which caused excessive deflections. It was then decided to reverse the procedure, i.e., bring the model to power then start the tunnel. A close check had to be maintained on the transmission because of the heating problem, but as time went on, the transmission heating was gradually reduced. This method of operation proved to be successful and was used throughout the remainder of the test program.

Failure Number 2 occurred when the circuit breaker controlling the hydraulic pump kicked out, causing the model r.p.m. to suddenly drop before the tunnel could be stopped. This, essentially, set up the same conditions as those which occurred at the time of the first failure. Again the two blades in the upper rotor were badly damaged and another quantity of pressure probes were also damaged. At this time, it became necessary to cease test operations at GAC and transfer the model to the University of Detroit. The two subsequent blade failures occurred because of foreign matter passing through the blades and were not caused by any operational procedure or inherent feature of the concept itself. One substantiating bit of evidence that none of the blade failures were due to any inherent fault in the concept was the fact that no damage was suffered by the blades in the uninstrumented half of the model. Both rotors were identical in terms of construction and blade arrangement. The difference lay in the fact that it was necessary to install pressure measuring instrumentation close to the plane of the rotors, and that this was done on one half of the model only. The installation

14

GOODYEAR
AIRCRAFT

of the instrumentation reduced some of the clearances that normally
would have been present and which were present in the uninstrumented
half. On the basis of this evidence, it has been concluded that
the blade failures occurred because of test operational procedures
which induced unusual loading conditions on the blades, and by
foreign matter present in the tunnel passing through the blades.
The blade failures did not occur because of any fault in the con-
cept.

The curves of Figures 21 and 22 were developed from the following
analytical approach.

Jet efficiency was defined as

$$\eta_J = \frac{2 \; V_0}{V_0 + V_J} \qquad \text{where } V_0 = \text{Free Stream Velocity}$$
$$V_J = \text{Jet Velocity}$$

$$V_J = 2\left[\frac{(q_t + \Delta q_H)}{\rho}\right]^{\frac{1}{2}} \qquad \text{where } q_t = \text{Tunnel Dynamic Pressure in } \#/ft^2$$

$$\Delta q_H = q_e - q_1$$

$$q_e = \text{Dynamic pressure at exit nozzle in } \#/Ft^2$$

$$q_1 = \text{Dynamic pressure at inlet in } \#/FT^2$$

Internal flow efficiency was given by

$$\eta_i = \frac{Q_F \times \Delta q_H}{550 \times HP \text{ in.}}$$

$$\text{where } Q_F = A_e \, V_e \text{ and } A_e = \text{Exit Nozzle area in } Ft^2$$

$$V_e = \text{Velocity of airstream at the exit nozzle}$$

$$V_e = \sqrt{\frac{2 \; q_e}{\rho}}$$

overall propulsive efficiency

$$\eta = \eta_J \times \eta_i$$

$$q_e = \left(\frac{\sqrt{H_1 - P_1} + \cdots\cdots + \sqrt{H_n - P_n}}{n} \right)^2$$

$$H = \text{Total Head in } \#/\text{Ft}^2$$

$$P = \text{Static Head in } \#/\text{Ft}^2$$

The curves in Figure 23 are based on the following definitions:

F_{100} = Thrust when doors are 100% open and the model is in the hovering condition.

F_n = Thrust vector obtained when doors are in any intermediate position including full closed.

$\dfrac{F_n}{F_{100}}$ = $\dfrac{\text{Thrust vector obtained in transition}}{\text{Hovering thrust}}$

B. EXTERNAL AERODYNAMICS

The same model that was tested at the Goodyear tunnel to obtain the internal flow characteristics was taken to the University of Detroit wind tunnel to investigate its external force properties. This model was a flexible configuration capable of simulating varying flight conditions. Modifications were possible in (1) rotor blade angle, θ, (2) Variation of inlet and exit area by varying top and bottom doors, ϕ. and (3) Variation in rotor power and RPM. When mounted in the tunnel further variations in angle of attack and forward flight speed could be simulated.

The scheduled test plan was based on two weeks of data collection, however, due to the long installation and a model blade failure, the actual data collection time was reduced to one week. The model blade failure also required a change in the preplanned blade configuration from coaxial operation-4 blades to single axial operation-2 blades. This change seriously effects the blade activity factor as well as permits higher rotational losses. Because of the extensive number of variables and the complexities in model changes, only a small portion of the anticipated points could be run. On the spot moderation of the test runs was relied on to assure coverage of the most effective parameters. As a result of this situation it was necessary to choose between running in or out of ground effect although both were scheduled. Since installation of the ground board would have resulted in further delay, it was decided to run out of ground effect. Upon return of the model to GAC where further internal flow tests were conducted, it was possible to obtain limited data in the hovering condition in ground effect.

16

The ratio of ground distance to rotor diameter $\frac{Z}{D}$ used in obtaining this data was .77. Analysis of the data revealed that the rotors operate more efficiently in ground effect as shown in Figures 30 and 31, but sufficient data was not available to correlate this effect with the external forces acting on the model, since use of the force system in the GAC tunnel was not possible. It is, therefore, concluded that more complete tests will be necessary before any trends or significant conclusions can be established.

The measurements taken at the University of Detroit were the lift, moment, the resultant horizontal force (T_H-D_M), and rotor torque. Investigations were also made to evaluate the effect of some minor components. (1) Hovering with and without the doors was investigated. (2) In forward flight the effect of vanes (doors) vs. plates was obtained. (3) A tail-on, tail-off run was made to evaluate the effect of the installed tail. (4) Special runs were made to obtain the drag-lift polar at high speed, without model power.

During the initial testing it was found that the magnitude of thrust obtained was far less than expected due to the limiting factors mentioned above. Since negative thrusts were not a realistic flight condition, the tunnel velocity was limited to a speed at which (T_H-D_M) was only slightly negative. A tabulation of the test runs investigated at the University of Detroit are presented in Table II, Figure 32.

Reference 7, which was used in the following evaluation of the external tests, is a factual presentation of measured values obtained in the University of Detroit wind tunnel.

1. Polars

To appraise the external efficiency of the unpowered model, lift and drag measurements were made to develop the polar curves for the system. These runs were made without model power and with plates on to represent the doors in the closed position. The inlet and exit were not faired in, so that data obtained can only be viewed from the standpoint of what would be happening under gliding conditions. Data was collected at two forward flight velocities of approximately 50 and 100 MPH. Figures 33 and 34 show the curves developed from the measured data. Included for comparison are two conditions using model power. It can be seen that with the application of power, increase of lift and decrease in drag can be expected. The substantial change in forces shown may be attributable in part to free stream flow existing in the internal system, thus changing the drag. There was not sufficient time to investigate the effect of directing the exit flow into the wake of the model. Past experience with similar installations of this nature have indicated that substantial improvement in the lift and drag of the body can be realized if close

attention is paid to feeding the exit flow into the wake. This
could probably best be done by a form of variable area exit nozzle.

Due to the complexity of eliminating the tare drag of the mounting
system from the tunnel measurements, no corrective runs were made.
Instead an approximate tare drag was computed for the strut system
with increases applied for the interference effects. A tare correc-
tion of .083 was used. The polar curve based on a corrected C_D is
shown in Figure 35. Although the curve as presented does not re-
flect a highly efficient lifting surface, external modifications
will prove beneficial in increasing the lift, while powered operat-
ion will have the effect of decreasing the true external drag, thus
improving the efficiency of the external lifting surface.

A special test run was made to evaluate the effect in drag of plates
vs closed doors. This condition would occur at high forward speeds.
It was found that when the doors were in place the drag was reduc-
ed slightly over the drag of the smooth plates, possibly due to
leakage of air in and out of the system, which created some boundary
layer control.

2. Hovering

Shown in Figure 36 are the results of the hovering flight analysis.
The direct lift readings obtained during the test were divided by
the model disk area to yield an operating disk loading T/A. During
each test run, measurements of torque on the rotor shaft were taken.
Presented in Figure 37 is the measured torque represented as model
horsepower varying with RPM and blade angle. From the measured
lift and horsepower the power loading T/HP can be obtained.

From Figure 36 it can be seen that the configuration tested exhib-
its reasonable hovering capabilities at optimum disk loadings. Good
helicopter rotor design is expected to yield figures of merit in
the order of 0.7. The configuration tested is yielding an $M = 0.5$.
It was necessary at the onset of the University of Detroit tests
to modify the rotor configuration from four blades - coaxial, and
counter-rotational to two blades single rotation. Increasing the
activity factor to two, four or six blade operation and including
co-axial operation of both rotors to reduce rational losses,
could increase the figure of merit to between 0.6 and 0.7 at optimum
disk loadings. This hovering efficiency if realized should bring
the attainable value to that assumed in the proposed test bed design.
Although the model test indicates that a decrease in hovering effic-
iencies occurs with increasing disk loading, this decrease in eff-
iciency which increases the power required, can be compensated for
by an increased number of blades with optimum blade design.

A special run was made to evaluate the effect of having the doors
in the flow during hover. Comparing runs at high blade angle, re-
moval of the doors increased the obtainable lift approximately 5%.
This value shows good correlation with the results obtained from the
internal flow tests.

18

3. Forward Flight and Transition

From the lift and resultant horizontal force, T_H-D_M, obtained from the University of Detroit force tests, a picture of the forward flight and transition history can be determined. The resultant force, (T_H-D_M) when plotted against velocity (q) yields the speed for equilibrium flight (A) and from the lift vs velocity, the lift obtained for that flight speed may be determined (B). Since no tare drag measurements were made at Detroit, an approximate correction to account for struts and interference was made and applied to the (T_H-D_M) curves.
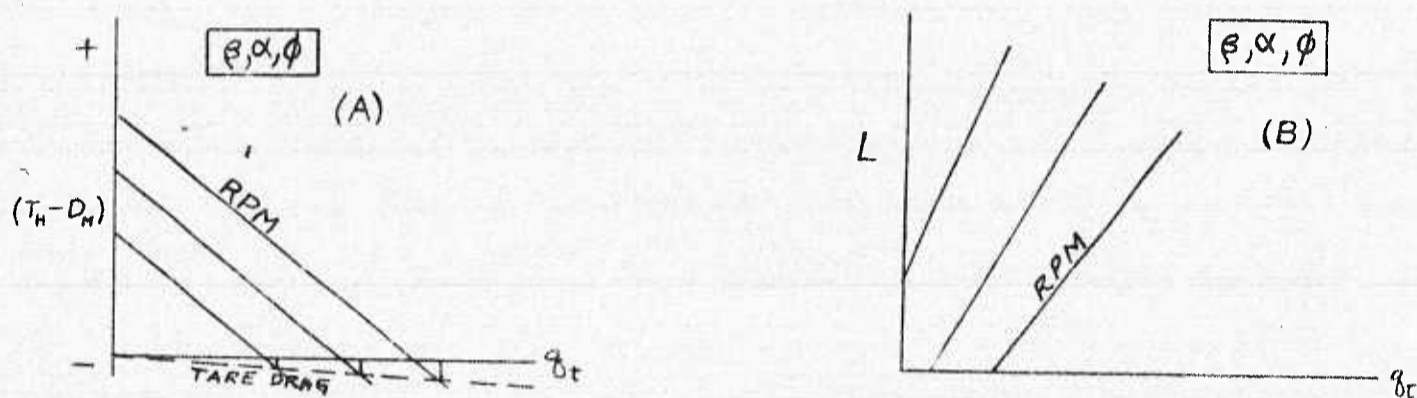
After searching the recorded data and plotting all continuous readings as above, a tabulation of equilibrium conditions can be made for each blade angle β at constant α showing equilibrium speed and lift at each door opening ϕ and rotor RPM. The use of lift coefficients for this determination was abandoned since C_L becomes infinite as velocity goes to zero. This would indicate an abnormally high horsepower in the transition flight range. Knowing the model disk area, a plot of RPM vs disk loading can be made from the tabulated data (C). Since some door openings were not tested a cross plot of the above curve was used to determine the dotted line on the RPM curve.

From the tabulated equilibrium data a plot of velocity vs RPM can also be made (E). Superimposed upon this speed chart are curves of constant disk loading or lift as obtained from the curve of T/A vs RPM. (F)

GOODYEAR
AIRCRAFT
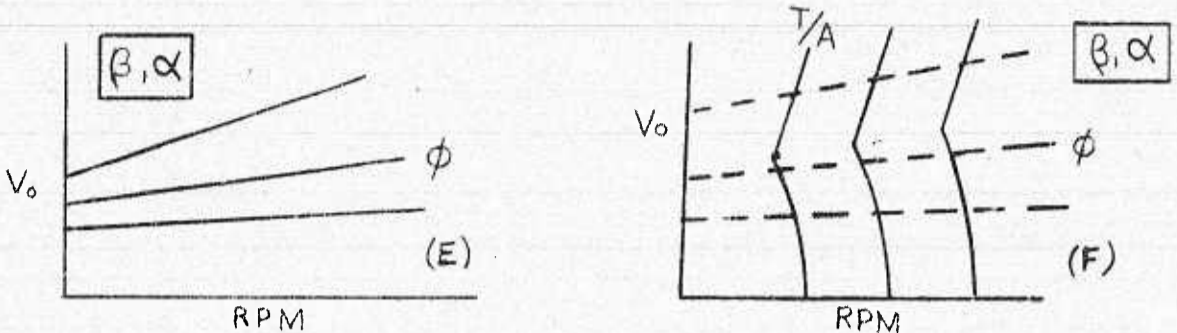
During the tests at The University of Detroit, values of blade torque were recorded and later transferred to rotor shaft horse-power vs RPM as shown in Figure 37. For a constant lift of the rotor, HP curves can be determined for the test bed.

Shown in Figures 38 (a) through 38 (d) are the fitted variation of disk loading with RPM showing the agreement with the test equilibrium points. Since the greatest number of continuous measurements were made at an attitude of -5°, all analysis is based primarily on this condition. A check of the scattered points collected at other rotor attitudes showed that some improvement in power required could be realized but these savings would occur at less desirable flight conditions.

The devloped horsepower vs velocity curve Figure 39 is expressed in full scale test bed horsepower. This scaling of horsepower from the model to full scale can be done by assuming that the model and full scale power coefficients are equal. This yields a power scale effect varying as the rotor diameters squared.

$$\text{HP full scale} = \text{HP model} \left[\frac{\text{D full scale}}{\text{D model}} \right]^2$$

The resulting curves Figure 39 indicate higher horsepowers than the preliminary design had anticipated but shows improved speed capabilities with lighter disk loadings.

An attempt was made to verify the reason for such high horsepower requirements by calculating the propulsive efficiency of the system. The propulsive efficiency is found by determining the power absorbed by the air and dividing it by the power supplied to the rotor.

The power into the rotor was measured in terms of torque on the rotor shaft during the wind tunnel test. These measurements are presented in Figure 37 in terms of blade angle and RPM.

GOOD/YEAR
AIRCRAFT

In evaluating the power absorbed by the air, thrust and velocity are required to compute horsepower. Measurments during the wind tunnel test did not evaluate pure thrust and drag but rather yielded the resultant horizontal force component. An estimate of the thrust can be gotten from the static conditions if it is assumed that the thrust did not vary with velocity. This assumption was determined to be somewhat optimistic since from the internal flow studies the thrust of the system appeared to decrease somewhat as speed increased.

From the curve of thrust variation with velocity, static thrust and equilibrium velocities can be obtained to determine the power absorbed by the rotor at various flight conditions.

Figure 40 presents the results of the calculated propulsive efficiencies. The deviation seen in the model efficiencies from that assumed in the estimated performance $(\eta = 0.65)$, explains part of the resultant high power requirements.

The speed increase due to lighter blade loadings are reasonable since the rotor can supply more thrust into speed rather than lift. Any extension of the solid line presented in the figure is limited in two ways. First, the rotor inlet area variation in testing was limited to a minimum of 25% inlet to disk area ratio; somewhere beyond this closure rotor blade starv'ng will occur and the horsepower will increase radically. Second, rotor tip losses will occur as tip speeds are increased over approximately 12,000 RPM. This also will result in an increase in HP.

Figure 39 represents the optimum operating blade angle for any disk loading. At lower disk loadings the curves for the Convoplane reflect a trend toward the typical helicopter operation. At higher loadings serious increases in horsepower occur during transition. At the time of the test arbitrary door settings were established to agree with those that were used in the previous internal flow studies. No attempt was made to optimize the door setting in order to see the improved effect on the force data. With a more thorough investigation, studying flow and forces, the horsepower during transition should be reduced and the curves approach those of a typical helicopter.

4. Stub Wing

With modification to the Convoplane test bed to optimize the internal and external flow, the system can be expected to exhibit improved horsepower demands with speed. The optimized curves of horsepower vs velocity, however, will still reflect the trend of Figure 39. A reduction in rotor loading will improve the speed potential of the vehicle.

To assist in the unloading of the rotor, aerodynamic surfaces might

GOOD$YEAR
AIRCRAFT

be utilized. All movable stub wings attached to the tips of the
rotor housing would affect this task. These wings should be op-
erated at near maximum lift in order to reduce the speed at which
they become effective. Operating at these lifts the wing absorbs
higher power than if operation were at (L/D_M) max, but in comparison
with the rotor power the wing demand is relatively low.

To appreciate the effect of a stub wing installation two wings
of an aspect ratio of 3 were theoretically applied to the test bed
configuration. Wing areas of 300 and 500 sq. ft. were applied to a
configuration having a gross weight of 7600 pounds.

T/A	Lift (Stub)	Wing Area 300 Ft²		500 ft²	
		Vel (MPH)	HP_R req'd	Vel MPH	HP_R Req'd
15 (completely loaded rotor)					
10	2510	57.2	46	44.3	36
8	3530	68.0	77	51.7	59
6	4550	76.5	112	59.8	88
4	5570	85.2	156	66.2	121
2	6582	92.6	197	71.8	153

Typifying the horsepower requirement above is the following curve.
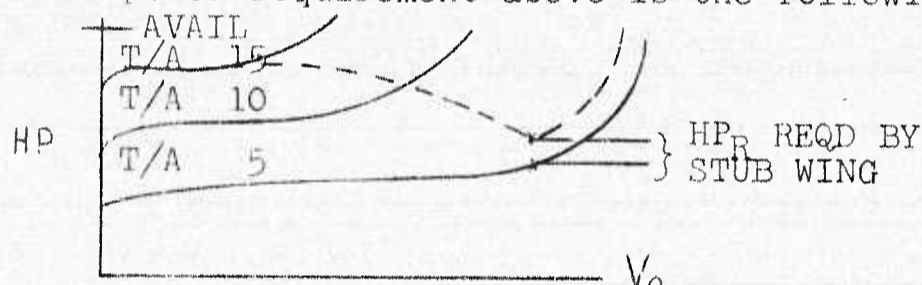
5. Longitudinal Stability and Control

As seen by reference to Figure 41, the model with horizontal tail
exhibits at any flight condition neutral to static negative pitch
stability. This then indicates an addition to the horizontal tail
area or an increase in its tail length is in order. Of greater con-
cern however, is the lack of ability of the existing horizontal tail
to trim-out the pitching moment. Figure 42 shows the pitching mom-
ent of the model with horizontal tail for equilibrium flight con-
ditions, i.e., when lift equals weight and thrust equals drag. From
the limited tail-off wind tunnel test data, and an estimate of the
maximum lift co-efficient of the horizontal tail, the pitching mom-
ent capability of the horizontal tail is defined in Figure 41 as
well. Those operating conditions below the capability curve can be
trimmed out in pitch; that area above the curve indicates the de-
ficiency of the horizontal tail.

This brief analysis of pitch stability and control indicates that
further effort must be expended, primarily by means of wind tunnel
tests, to achieve satisfactory characteristics over the entire flight
regime.

SECTION V.   CONCLUSIONS AND RECOMMENDATIONS

A. CONCLUSIONS

From the work accomplished so far, it may be concluded that a small penalty is being paid for the presence of doors and turning vanes in the vertical airflow. Despite this, hovering efficiencies approaching that of helicopters are being achieved.

In the forward flight regime the rotor appears to suffer no adverse flow; therefore an arrangement of rigid rotors with collective pitch control should produce reasonable forward flight propulsion.

It has been demonstrated that the buried rotor-shroud arrangement, which is the nerve center of the Convoplane concept, provides all the necessary flow conditions through turning of the air to produce hovering, transition and relatively high forward speeds.

It has also been demonstrated that with additional work the efficiency of the propulsion system can be greatly improved   The wind tunnel model selected for this investigation has the flexibility necessary for the collection of basic information and continued studies along these lines should be made.

B. RECOMMENDATIONS

Now that feasibility of the concept has been proven, it is recommended that further studies be made to approach more optimum conditions with the various components of the internal-external configuration. Specifically, the following items are recommended.

1.   Since no opportunity to investigate the leading edge inlet or the exhaust at the trailing edge was possible, it is very definitely felt that a better shaped inlet and exhaust nozzle, with perhaps variable area control, will improve the flow conditions.

2.   An attempt should be made to shape the rotor shroud in order to improve hovering performance.

3.   The use of boundary layer control in the rotor shroud should be investigated.

4. The selection of more optimum door settings to obtain better forward flight efficiencies and improved transition qualities should be studied, since the door settings selected for testing were quite arbitrary and it has been shown that improvement is possible in this area.

5. An attempt should be made to arrive at a more improved rotor blade shape and a better twist distribution.

6. It is believed that neither the number of blades or the optimum blade angle setting has been obtained, therefore, further study is warranted in this area.

7. No attempt was made to improve the turning vanes either as to shape, number, or location. This area should receive further evaluation.

8. The power-off polar curves indicate that effort to improve the external configuration is warranted.

9. Additional horizontal tail area or tail length to that represented by the model will be necessary to assure static longitudinal stability. The problem of inadequate pitch control exists with the model configuration at low speeds. A continuing study is necessary to devise means of pitch control from hover to the maximum flight speed.

10. An improvement in the external lifting efficiency will permit the Convoplane to have a higher speed potential. The improvement may come from any means of reducing the rotor disk loading such as obtaining higher lift from the rotor housing or the incorporation of stub wings.

The wind tunnel model as tested was evolved with but meager information and heavy dependence for its modification for improvement was placed on the internal flow investigation. The curtailment of the internal flow investigation, due in part to mechanical difficulties, prevented any optimization of the configuration.

It is firmly believed that significant improvements can now be made in the recommended areas for further investigation. These studies can be made during the preliminary design phase for the flying test bed and incorporated in the full scale model before the detail design in initiated since the basic configuration is now established and the areas discussed would not appreciably change the status of this.

Since the feasibility of the Convoplane concept has now been demonstrated, it would be well to point out what this means in terms of

future application for this particular vehicle. Here we have an
aircraft with disk loadings and a hovering efficiency which approach-
es that of a helicopter. In addition, it should have the forward
flight stability of a conventional airplane. All in all, the
vehicle exhibits excellent growth potential.

With the rotors buried as they are within the wing, it will be
quite possible to operate in congested or partially cleared areas.
Furthermore, when it is necessary to lift and transport heavy loads
for short distances, the Convoplane with flat endplates at the wing
tips provides a means of attaching several units together to become
a form of flying crane for this purpose. A corollary to this appli-
cation is the fact that several units may be towed to a pre-determin-
ed location in a ferrying mission; then cut loose to land by them-
selves, or they may perform another mission such as rescue and then
be towed back. The function just described is possible since it
is an extension of a safety feature of the Convoplane, wherein, if
engine failure occurs, the vehicle may be glided to a safe landing.
This feature is made possible because of the fact that the Convo-
plane possesses a low wing loading.

The configuration is such that its final form can range from the
smaller reconnaissance type airplane to the larger cargo carrying
type of aircraft. It also exhibits possiblities of having STOL
capabilities as well as VTOL.

It is therfore recommended that a program be initiated for the
design and fabrication of a flying test bed, which would incorpor-
ate the features of the Convoplane. By means of this test bed, it
will be possible to obtain full scale free flight test data which
would be directly applicable to prototype designs for specific
missions. Information on stability, controllability, and general
flight performance during hovering, transition and full forward
flight will be obtained in true scale and would permit a realistic
evaluation of Convoplane potential for Army uses.

SECTION VI. REFERENCES

1. "Aerodynamics of Propulsion", Kuechmann and Weber McGraw-Hill Book Co., Inc. 1953

2. Schlichting, H., "Problems and Results of Investigations of Cascade Flow", J.I.A.S., March, 1954, pp 163 - 178.

3. ANC-9, Aircraft Propeller Handbook, Sept., 1956

4. McCoy, H. M. "Counter-Rotating Propellers", J.R.A.S. June, 1940, pp 481-498

5. Parlett, L. P. "Aerodynamic Characteristics of a Small Scale Shrouded Propeller at Angles of Attack" NACA TN 3547, Nov. 1955.

6. Platt, Jr., R. J. "Static Tests of a Shrouded and Unshrouded Propeller, NACA RM L7H25 February 9, 1948

7. Davenport, E. L. Jr., "Wind Tunnel Test - Goodyear Aircraft Convoplane" University of Detroit Aeronautical Laboratory March, 1958

Figure 1 Cross-Section Showing Model in Forward Flight Attitude

Figure 2 Cross-Section Showing Model In Hovering Attitude

Figure 3 Estimated Horsepower Required To Hover
vs. Gross Weight. (Proposed Convoplane Test Bed)

Figure 4 Estimated Effect of Rotor Diameter on
Horsepower Required (Proposed Convoplane Test Bed)

CONFIDENTIAL

Figure 5 Estimated Rotor Diameter Effect on Lift
and Horsepower (Proposed Convoplane Test Bed)

Figure 6 Estimated Variation of Shaft Horsepower
With Velocity (Proposed Convoplane Test Bed)

Figure 7 Three-View of Proposed Convoplane Test Bed

Figure 8 Front View of Model with Upper Doors and
Nose Fairing Removed. (GAC Wind Tunnel)

34

GOOD/YEAR
AIRCRAFT

GER 8763, REV. B.
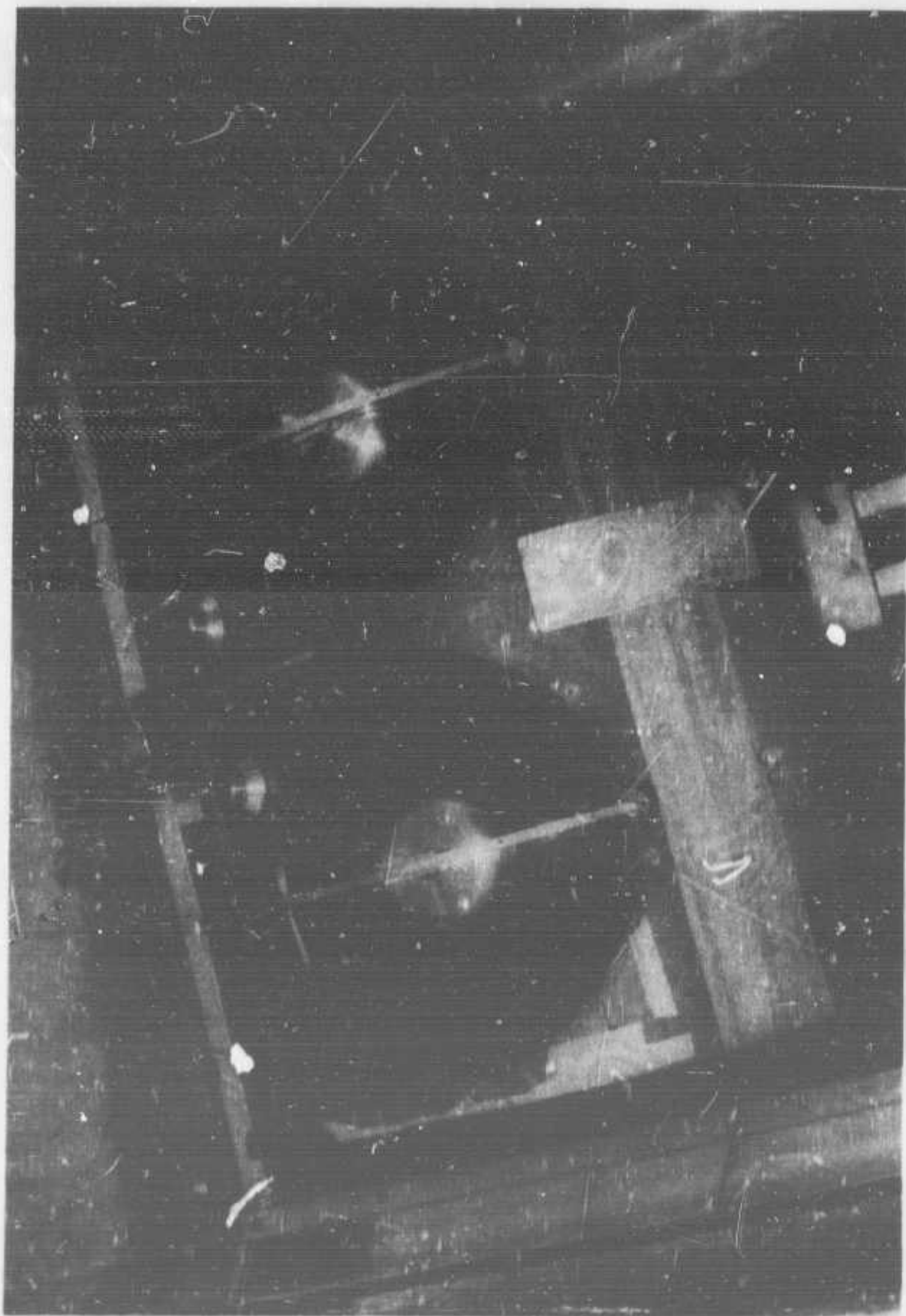
Figure 9. Top View of Model with Upper Doors Removed,
Showing Upper Turning Vanes. (GAC Tunnel)

Figure 10 Bottom View of Model with Lower Doors Removed, Showing
Lower Turning Vanes and Exit Total & Static Pressure Rake.
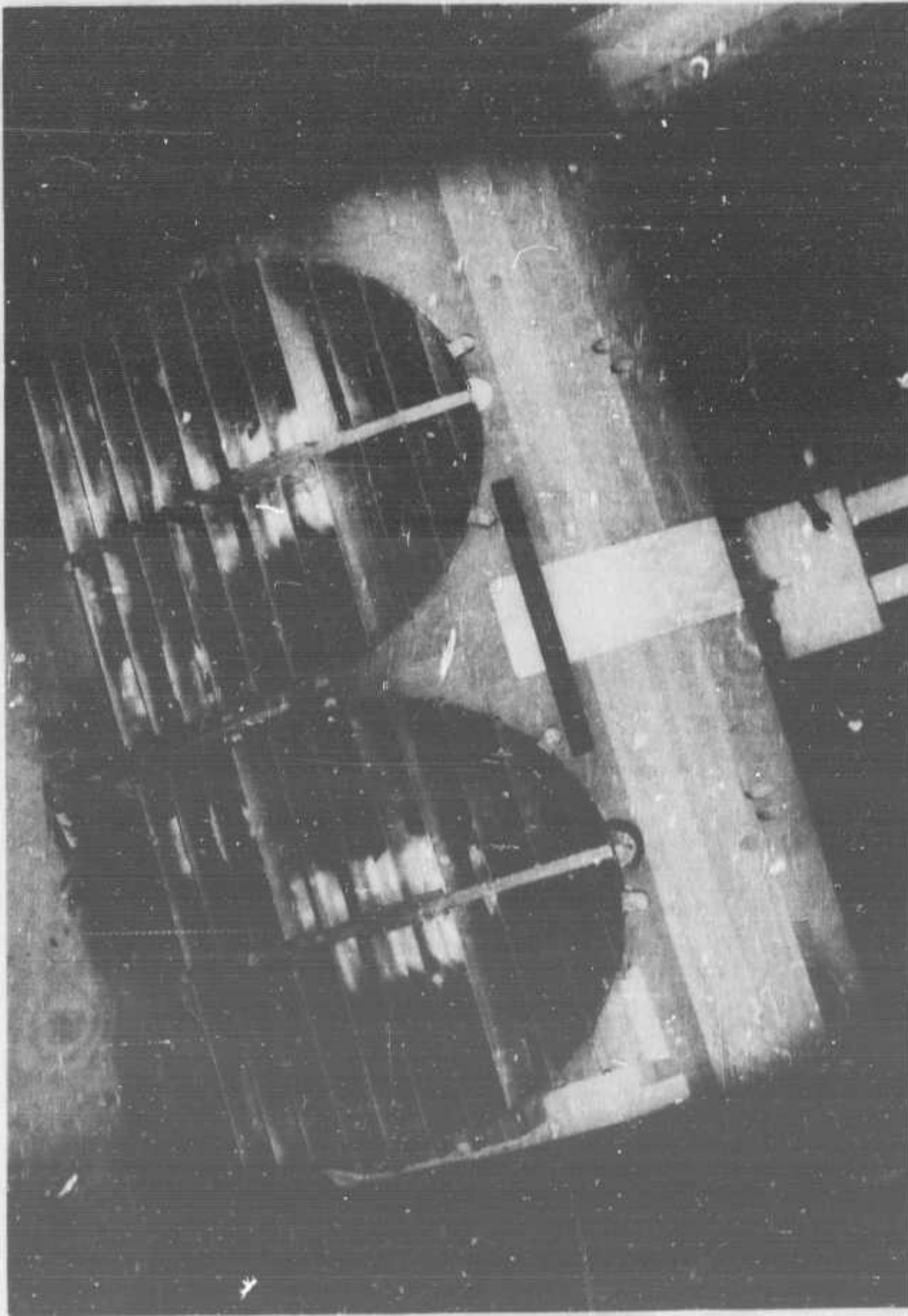
Figure 11 Top View of Model with Upper Doors
in Hovering Position (GAC Tunnel)
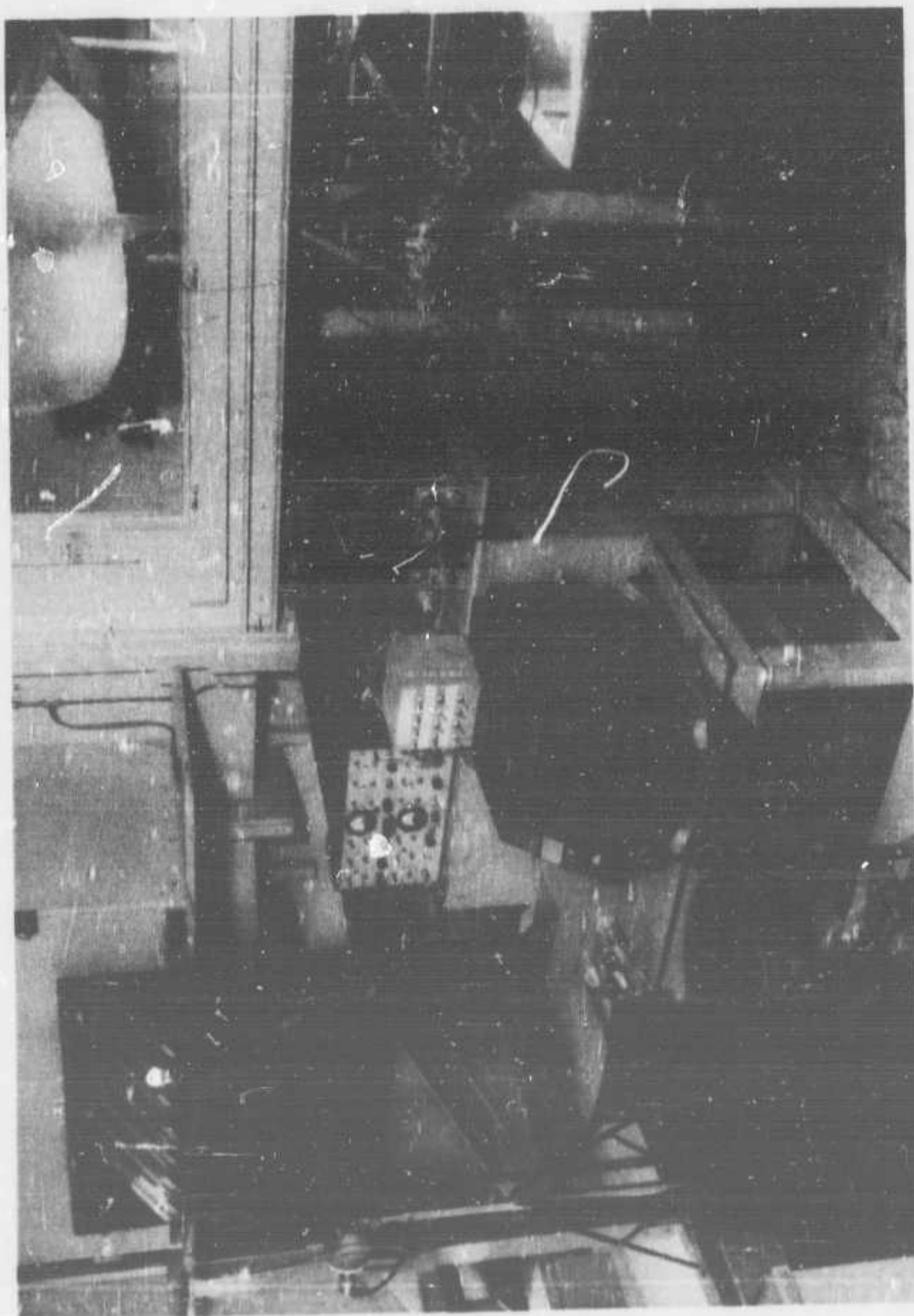
Figure 12 Pressure and Torque Measuring Equipment
(Oscillograph, Scana-Valves & Balance Box)

Figure 13 Pressure Measuring Equipment -
50 Tube Manometer Bank.

Figure 14 View Showing Top Doors in Forward Flight
Position (University of Detroit Tunnel)

Figure 15 Three-Quarter Front View of Convoplane
Model (University of Detroit Tunnel)

Figure 16 Three-Quarter Front View Showing Plates Instead of
Doors in Forward Flight Position. (U. of D. Tunnel)

Figure 17 Rear View of Model Showing Empennage and
Exit Duct. (University of Detroit Tunnel)

Figure 18 Power Loading Vs. Disk Loading
(Convoplane Model Tests)

FIGURE OF MERIT AS A FUNCTION OF POWER LOADING AND DISK LOADING USING VARIOUS ROTOR CONFIGURATIONS

DOORS OUT
UPPER TURNING VANES OUT
BLADE ANGLE = 10°

IDEAL HOVERING EFFICIENCY M 1.0

o – 2-BLADED ROTOR – SINGLE ROTATION
△ – 4-BLADED ROTOR – SINGLE ROTATION
□ – 2-BLADED ROTOR – COUNTER-ROTATION

POWER LOADING – #/HP = $\frac{I}{HP}$

DISK LOADING – #/FT^2 = $\frac{I}{A}$

Figure 19 Power Loading vs. Disk Loading
(Convoplane Model Tests)

Figure 20 Measured Horsepower Supplied to
Rotors (Convoplane Model Tests)

Figure 21 Efficiency vs. Advance Ratio
(Convoplane Model Tests)

Figure 22 Efficiency vs. Advance Ratio
(Convoplane Model Tests)

Figure 23 Variation of Thrust Vector With Door
Opening (Convoplane Model Tests)

Figure 24 Pressure Tap Locations
(Convoplane Model Tests)

2-BLADES
COUNTER-ROTATING
$\beta = 10°$
AREA RATIO 25% (A_i/A)
$q_o = 46.7$ P.S.F.
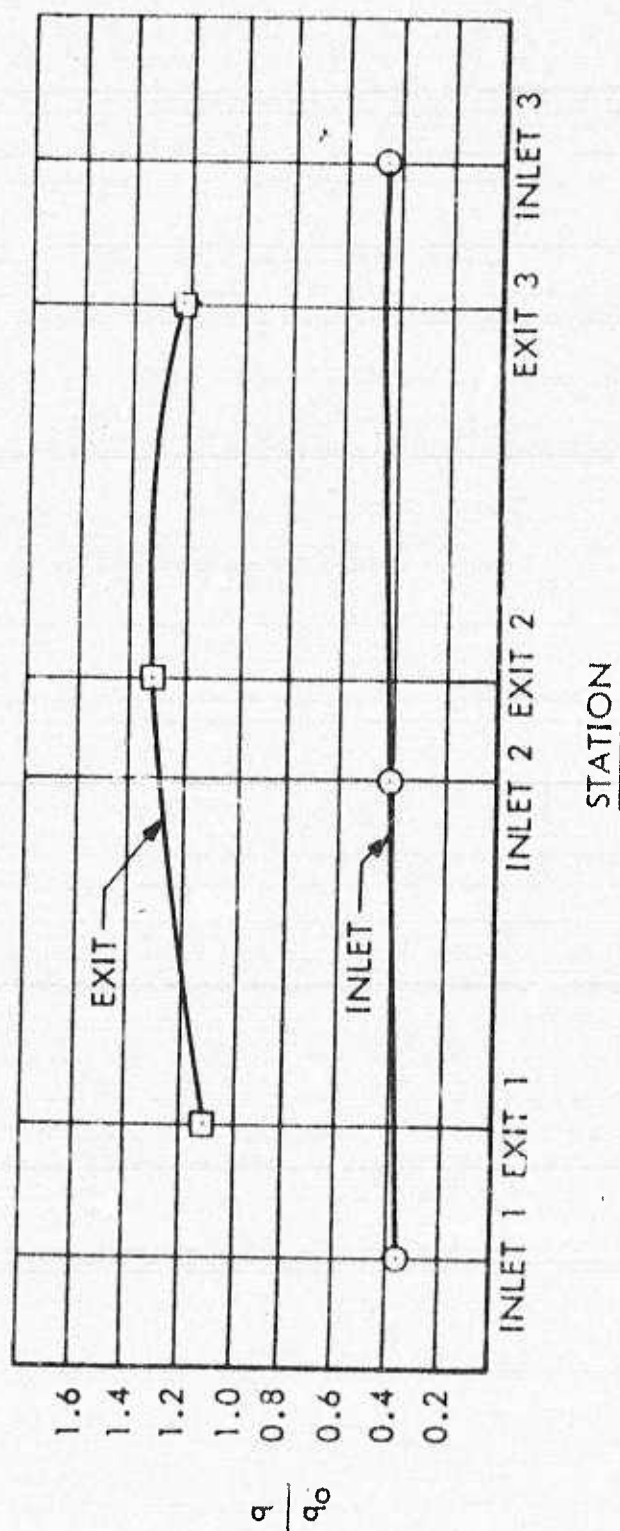
Figure 25 Pressure Distribution vs. Station (Inlet
and Exit) (Convoplane Model Tests)

Figure 26 Pressure Distribution vs. Rotor Station
(Convoplane Model Tests)

2-BLADES
COUNTER-ROTATING
$\beta = 10°$
25% AREA RATIO (A_f/A)
$q_o = 46.7$ P.S.F.
5000 RPM
BELOW ROTOR

Figure 27 Pressure Distribution vs. Rotor Station
(Convoplane Model Tests)

Figure 28 Variation of Pressure With
Blade Angle (Convoplane Model Test)
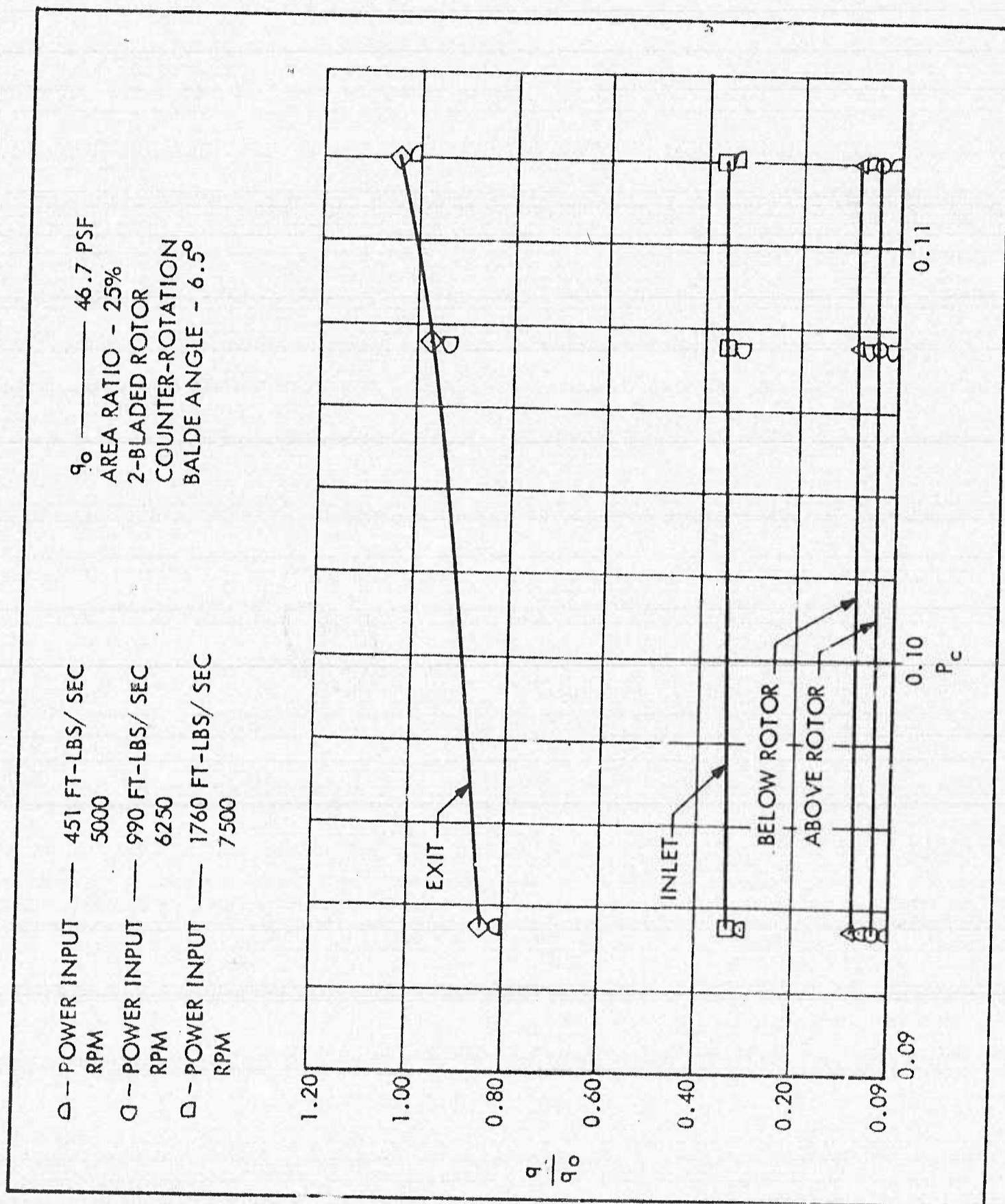
Figure 29 Variation of Pressure With
Power Input (Convoplane Model Tests)

CONFIDENTIAL

Figure 30 Power Loading vs. Disk Loading (in and out of
Ground Effect) (Convoplane Model Tests)

Figure 31 Power Loading vs. Disk Loading (in and out of Ground Effect) (Convoplane Model Tests)

RUN	β	φ %	α	A V=0 fPs -10 -5 0 5 10	B V=25.8 fPs -10 -5 0 5 10	C V=36.3 fPs -10 -5 0 5 10	D V=44.6 fPs -10 -5 0 5 10	E V=51.4 fPs -10 -5 0 5 10	G V=57.5 fPs -10 -5 0 5 10	F V=62.7 fPs -10 -5 0 5 10
I	2.5°	25	PLATES	x x x x x	x x x x x	x x x x x	x x x x x			
I		25	VANES		x x	x x	x			
		50								
III		75			x x x	x x x x		x x x		
II		100			x x x	x x x				
	10°	25								
V		50			x		x x x		x	
IV		75			x		x x x	x		x
VI		100			x	x x				
XII	15°	25		x x x			x			x TAIL ON
X		50			x		x x			x TAIL OFF VIII F
VIII		75			x		x x x			x
VII		100			x	x x				
XI		100 OFF			x					
	20°	25								
XIV		50			x		x			x
		75								
		100								
		100 OFF			x					
SPEC	2.5°	25		x x x x x						
SPEC	2.5°	25		x x x x x						

At 50 & 100 MPH

OFF DOORS OFF

FAN SPEED FOR VARIOUS BLADE ANGLES

β = 2.5°	β = 10°	β = 15°	β = 20°
5000	5000	5000	5000
7500	7500	7500	7500
9000	9500	8500	
10200			

Figure 32 Table 2 University of Detroit Test
Runs. (Convoplane Model Tests)

Figure 33 Polar Runs (C_L vs. a)
(Convoplane Model Tests)

$\phi = 2.5\%$

Figure 33 Polar Runs (C_D vs. a)
(Convoplane Model Tests)

Figure 35 Polar Runs (C_L vs. C_D) High Speed Flight
Condition No Power (Convoplane Model Tests)

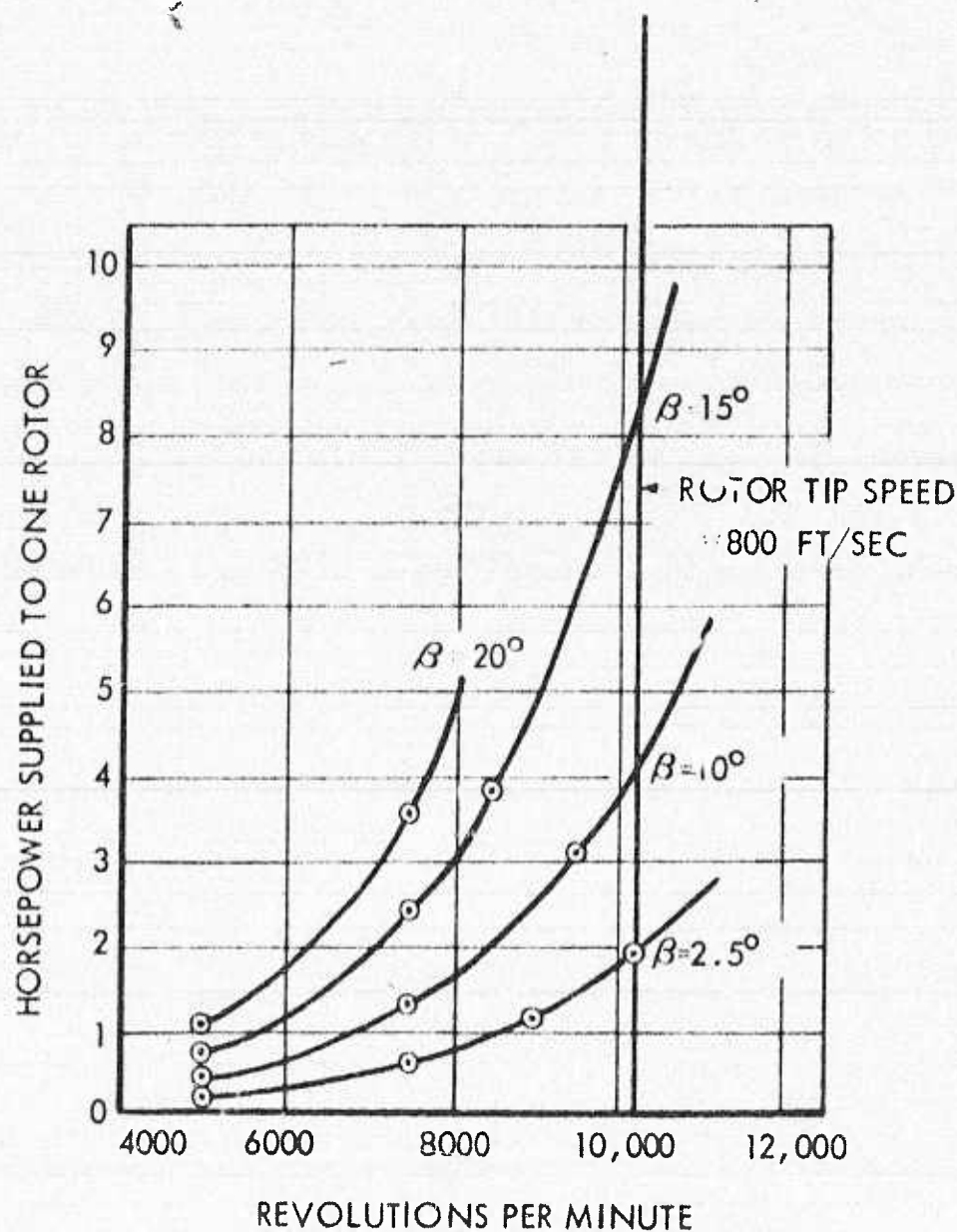Figure 36 Variation of Hovering Efficiency with Disk
Loading and Power Loading (Convoplane Model Tests)

Figure 37 Measured Model Horsepower Supplied To
The Rotor (Convoplane Model Tests)

Figure 38 Variation of Disk Loading With R.P.M. Approximated
Curves From Test Measurements (Convoplane Model Tests)

Figure 39 Full Scale Horsepower Required vs. Velocity For
Various Disk Loadings. (Convoplane Model Tests)

Figure 40 Efficiencies At Equilibrium Flight
(Convoplane Model Tests)

Figure 41 Pitching Moment vs. Angle of
Attack. (Convoplane Model Tests)

Figure 42 Pitch Trim Capability
(Convoplane Model Tests)

LIST OF SYMBOLS

S	=	Wing Area (Ft^2)
T	=	Hovering Thrust (Lbs)
T_H	=	Forward Thrust (Lbs)
V_O	=	Free Stream Velocity (MPH)
V_J	=	Jet Velocity
V_E	=	Velocity of Airstream at Exit Nozzle
W_O	=	Gross Weight (Lbs) (Full Scale)
C_L	=	Wing Lift Coefficient
C_D	=	Wing Drag Coefficient
C_M	=	Pitching Moment Coefficient
a	=	Wing Angle of Attack
β	=	Rotor Blade Angle Setting
η	=	Overall Populsive Efficiency
η_J	=	Jet Efficiency
η_1	=	Internal Flow Efficiency
ρ	=	Air Density (Slugs/Ft^3)
$\emptyset$	=	Top and Bottom Door Opening Positions

25% Door Opening = $\dfrac{A_1}{A}$ = 25%

50% Door Opening = $\dfrac{A_1}{A}$ = 50%

75% Door Opening = $\dfrac{A_1}{A}$ = 75%

* Balance of Symbol's on Page vii, pull out when reading text.

UNCLASSIFIED

205773-1

Armed Services Technical Information Agency

ARLINGTON HALL STATION
ARLINGTON 12 VIRGINIA

FOR

MICRO-CARD

CONTROL ONLY

2 OF 2

NOTICE: WHEN GOVERNMENT OR OTHER DRAWINGS, SPECIFICATIONS OR OTHER DATA
ARE USED FOR ANY PURPOSE OTHER THAN IN CONNECTION WITH A DEFINITELY RELATED
GOVERNMENT PROCUREMENT OPERATION, THE U. S. GOVERNMENT THEREBY INCURS
NO RESPONSIBILITY, NOR ANY OBLIGATION WHATSOEVER; AND THE FACT THAT THE
GOVERNMENT MAY HAVE FORMULATED, FURNISHED, OR IN ANY WAY SUPPLIED THE
SAID DRAWINGS, SPECIFICATIONS, OR OTHER DATA IS NOT TO BE REGARDED BY
IMPLICATION OR OTHERWISE AS IN ANY MANNER LICENSING THE HOLDER OR ANY OTHER
PERSON OR CORPORATION, OR CONVEYING ANY RIGHTS OR PERMISSION TO MANUFACTURE,
USE OR SELL ANY PATENTED INVENTION THAT MAY IN ANY WAY BE RELATED THERETO.

UNCLASSIFIED